The Recent Partial Recovery in Sahel Rainfall: A Fingerprint of Greenhouse Gases Forcing?

Article · November 2015

11 authors, including:

Serge Janicot
Pierre and Marie Curie University - Paris 6

Marco Gaetani
Pierre and Marie Curie University - Paris 6

Alessandra Giannini
Columbia University

Michela Biasutti
Columbia University

Derber, J.C., D.F. Parrish and S.J. Lord, 1991. The new global operational analysis system at the National Meteorological Center. *Weather Forecasting*, 6, 538–547.

Entekhabi et al., 2010. The Soil Moisture Active Passive (SMAP) mission–*Proceedings of the IEEE*, 98, 704-716.

Funk, C.C., P.J. Peterson, M.F. Landsfeld, D.H. Pedreros, J.P. Verdin, J.D. Rowland, B.E. Romero, G.J. Husak, J.C. Michaelsen and A.P. Verdin, 2014. A quasi-global precipitation time series for drought monitoring: U.S. Geological Survey Data Series 832, 4 p.. *http://dx.doi.org/10.3133/ds832*.

Getirana, A.C.V., A. Boone, D. Yamazaki, B. Decharme, F. Papa and N. Mognard, 2012. The Hydrological Modeling and Analysis Platform (HyMAP): Evaluation in the Amazon basin. *J. Hydrometeorol.* 13, 1641–1665, doi: 10.1175/JHM-D-12-021.1.

Kolars, J., 1994. Problems of international river management: The case of the Euphrates. *International Waters of the Middle East—from Euphrates–Tigris to Nile*. Oxford University Press, London, 44-94.

Koster, R.D., M.J. Suarez, A. Ducharne, M. Stieglitz and P. Kumar, 2000. A catchment based approach to modeling land surface processes in a general circulation model: 1. Model structure, *J. Geophys. Res. Atmos.*, 105, 24809–24822, doi:10.1029/2000JD900327.

Kumar, S.V., C.D. Peters-Lidard, Y. Tian, J. Geiger, P.R. Houser, S. Olden, L. Lighty, J.L. Eastman, P. Dirmeyer, B. Doty, J. Adams, E.F. Wood and J. Sheffield, 2006. LIS – An interoperable framework for high resolution land surface modeling. *Environ. Modell. Softw.*, 21, pp 1402-1415.

Liu, Y., R. Parinussa, W. Dorigo, R. De Jeu, W. Wagner, A. Van Dijk, M. McCabe and J. Evans, 2011. Developing an improved soil moisture dataset by blending passive and active microwave satellite-based retrievals. *Hydrol. Earth Syst. Sci.*, 15, 425-436.

Niu, G.-Y., Z.-L. Yang, K.E. Mitchell, F. Chen, M.B. Ek, M. Barlage, L. Longuevergne, A. Kumar, K. Manning, D. Niyogi, E. Rosero, M. Tewari and Y. Xia, 2011. The community Noah land surface model with multiparameterization options (Noah-MP): 1. Model description and evaluation with local-scale measurements. *J. Geophys. Res.*, doi:10.1029/2010JD015139.

Reichle, R.H., R.D. Koster, G.J.M. De Lannoy, B.A. Forman, Q. Liu, S.P.P. Mahanama, and A.Touré, 2011. Assessment and Enhancement of MERRA Land Surface Hydrology Estimates. *J. Clim.*, 24, 6322–6338. doi: *http://dx.doi.org/10.1175/JCLI-D-10-05033.1*

Salmon, J. M., M.A. Friedl, S. Frolking, D. Wisser, and E.M. Douglas, 2015. "Global rain-fed, irrigated, and paddy croplands: A new high resolution map derived from remote sensing, crop inventories and climate data." *Int. J. Appl. Earth Obs. and Geoinf.*, 38: 321-334

Savoca, M.E., G.B. Senay, M.A. Maupin, J.F. Kenny and C.A. Perry, 2013. Actual evapotranspiration modeling using the operational Simplified Surface Energy Balance (SSEBop) approach: U.S. Geological Survey Scientific Investigations Report 2013-5126, 16 p., *http://pubs.usgs.gov/sir/2013/5126*.

Tapley, B., S. Bettadpur, J.C. Reis, P.F. Thompson and M.M. Watkins, 2004. GRACE measurements of mass variability in the earth system. *Science*, 305(5683), 503–505, doi:10.1126/science.1099192.

World Bank, 2006. Iraq: Country Water Resources Assistance Strategy: Addressing Major Threats to People's Livelihoods. Report No. 36287-IQ. Water, Environment, Social and Rural Development Department, Middle East and North Africa Region.

Zhan et al., 2011. Soil Moisture Operational Product System (SMOPS) algorithm theoretical basis document Version 3.0. *http://www.ospo.noaa.gov/Products/land/smops/figures/SMOPS_ATBD_v3.0.pdf*.

The Recent Partial Recovery in Sahel Rainfall: A Fingerprint of Greenhouse Gases Forcing?

Serge Janicot[1], Marco Gaetani[2], Frédéric Hourdin[3], Alessandra Giannini[4], Michela Biasutti[5], Elsa Mohino[6], Yongkang Xue[7], Aaron Boone[8], Amadou Gaye[9], Seyni Salack[10] and Christophe Lavaysse[11]

[1]Laboratoire d'Océanographie et de Climat: Expérimentations et Approches Numériques, Sorbonne-Universités, CNRS-IRD-UPMC-MNHN, Paris, France; [2]Laboratoire Atmosphères Milieux Observations Spatiales, Sorbonne-Universités, Paris, France; [3]Laboratoire de Météorologie Dynamique, Sorbonnes-Universités, Paris, France; [4]International Research Institute for Climate and Society, Columbia University, Palisades, NY, USA; [5]Lamont Doherty Earth Observatory, Columbia University, NY, USA; [6]Geophysics and Meteorology Department, Complutense University of Madrid, Spain; [7]Department of Atmospheric and Oceanic Sciences, University of California, Los Angeles, CA, USA; [8]Météo France, Centre National de Recherches Météorologiques–Groupe d'Etude de l'Atmosphère Météorologique, Toulouse, France; [9]Laboratoire de Physique de l'Atmosphère et de l'Océan–Siméon Fongang, Ecole Supérieure Polytechnique, Université Cheikh Anta Diop, Dakar, Sénégal;[10]Karlsruhe Institute of Technology, Institute of Meteorology and Climate Research, Atmospheric Environmental Research (IMK-IFU), Garmisch-Partenkirchen, Germany;[11]European Commission, Joint Research Centre, Ispra, VA, Italy

In the present context of climate transition under the influence of anthropogenic forcings, a critical issue is proper attribution of climate anomalies, in order to avoid misinterpretations leading to possible maladaptations. Over the last 60 years, the monsoon region of the Sahel has been coping with some of the most severe climate variability in the world, including two decades of persistent excessive rainfall in the 1950s–1960s, followed by two decades of rainfall deficits (see figure on page 12). Recently, there has been a partial recovery with annual rainfall amounts fluctuating around the long-term mean, more evident over the central Sahel than over the western Sahel (Lebel and Ali, 2009). The current period is also characterized by a deficit of rainy days with a rise in extreme rainfall occurrences, indicating the intensification of the hydrological cycle (Giannini et al., 2013; Panthou et al., 2014). This climate is drier in the sense of persistent dry spells compared to the 1950s–1960s, while at the same time there is an increased probability of floods.

While projections of future climate over the Sahel in Coupled Model Intercomparison Project Phase 5 (CMIP5) runs are quite uncertain in terms of rainfall regime (Biasutti, 2013), they are qualitatively consistent with this recent evolution: they show that at the end of the 21st century under the highest greenhouse gases (GHG) emission scenario, RCP8.5, a zonal rainfall anomaly dipole with more summer precipitation over the central Sahel (especially in August-September), and less summer precipitation (especially in June-July) over the west-

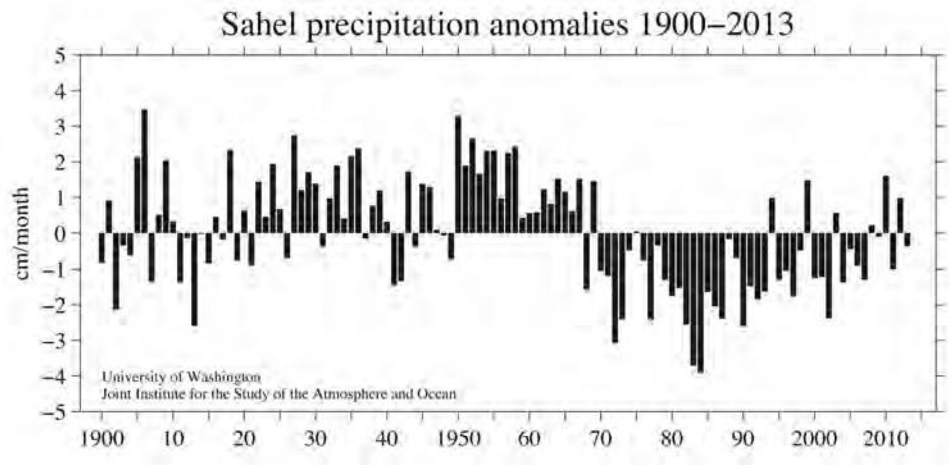

June–October averages over 20-10N, 20W-10E. NOAA/NCDC Global Historical Climatology Network data.

ern Sahel (Biasutti, 2013), is accompanied by an increase in the number of extreme rainfall days (Vizy et al., 2013).

Various studies have noted the importance of global sea surface temperature (SST) variability, land surface and GHG and aerosol concentrations, and how they may impact monsoon precipitation. Based on multi-model experiments including the latest CMIP5 results, a consensus is emerging on the drying effect of global SST, and the opposing positive effect of increasing GHG concentration (e.g., Haarsma et al., 2005; Held et al., 2005; Hoerling et al., 2006; Cook and Vizy, 2006; Caminade and Terray, 2010; Giannini, 2010; Biasutti, 2013; Bony and al., 2013; Gaetani et al., 2015).

Uncertainty in Climate Models Sensitivity to SST and GHG Forcings Over the Sahel

Recently, Dong and Sutton (2015) suggested that higher atmospheric concentrations of GHG and the direct increase in atmospheric temperature were primarily responsible for the Sahel rainfall recovery. Using the Hadley Centre Global Environment Model Version 3-A (HadGEM3-A), they simulated epochal climate changes for the period 1964–2011 under different idealized conditions and investigated the individual roles of global SST, GHG and atmospheric aerosol concentrations in driving the recent recovery of the monsoonal precipitation in the Sahel. They suggest that the direct influence of higher levels of GHG in the atmosphere is the main cause of Sahel rainfall recovery, with an additional role for changes in anthropogenic aerosol precursor emissions. They also found that recent changes in SSTs, although substantial, did not appear to have a significant impact on the recovery, and that rainfall is likely to be sustained or amplified in the near term.

By using only one model, it is not possible to evaluate the robustness of the results. Giannini (2015) showed how the HadGEM2-A underperforms in reproducing the effect of historical SST on Sahel rainfall compared to the ensemble of the other models available in CMIP5. Multiple data sets of numerical experiments were also analyzed and extracted from the recently available CMIP5 archive (Taylor et al., 2012) that simulate idealized conditions that are more or less similar to the ones used by Dong and Sutton (2015). The behaviors of 11 models were compared, including the HadGEM2-A (Table 1), and these were run in the atmosphere-only configuration. The monsoonal season from July to September (JAS) also analyzed.

First, the simulations of the 11 CMIP5 models (Table 1) forced by the observed global SST over the period 1979-2008 (control simulations, CTL) were analyzed. The long-term trends of Sahelian precipitation are affected by global SST variability, mainly through the differential heating in the Northern

Table 1. Models analyzed. CMIP5 model information and outputs are available through the Earth System Grid Federation Archive at: *http://cmip-pcmdi.llnl.gov/cmip5*.

Modeling Center	Model	Resolution Lat./Long.
Beijing Climate Center, China Meteorological Administration	BCC-CSM1-1	T42 (~2.8°)
Canadian Centre for Climate Modeling and Analysis	CanAM4	T42 (~2.8°)
Centre National de Recherches Météorologiques/Centre Européen de Recherche et de Formation Avancée en Calcul Scientifique	CNRM-CM5	T127 (~1.4°)
LASG, Institute of Atmospheric Physics, Chinese Academy of Sciences and CESS, Tsinghua University	FGOALS-g2	3.0° x 2.8°
Met Office Hadley Centre	HadGEM2-A	1.25° x 1.875°
Institut Pierre-Simon Laplace	IPSL-CM5A-LR	1.875° x 3.75
	IPSL-CM5B-LR	1.875° x 3.75
Atmosphere and Ocean Research Institute (The University of Tokyo), National Institute for Environmental Studies, and Japan Agency for Marine-Earth Science and Technology	MIROC5	T127 (~1.4°)
Max Planck Institute for Meteorology	MPI-ESM-LR	T73 (~1.9°)
	MPI-ESM-MR	T73 (~1.9°)
Meteorological Research Institute	MRI-GCCM3	T159 (~1.125°)

Hemisphere and the Tropics (Mohino et al., 2011; Giannini et al., 2013), and by the GHG radiative warming of the land surface, which is particularly important at the regional scale (Giannini, 2010; Gaetani et al., 2015). The sensitivity of the Sahelian rainfall was then compared to the differential heating of global SST to the response to land surface warming over North Africa. Indexes were defined for Sahelian rainfall (SRI), North Atlantic minus Global Tropical SST differential heating (NAT), and surface air temperature for North Africa (SAT). The SRI sensitivity to the changes in NAT and SAT shows that the HadGEM2-A is less sensitive to the SST differential heating and surface air temperature, with SRI versus

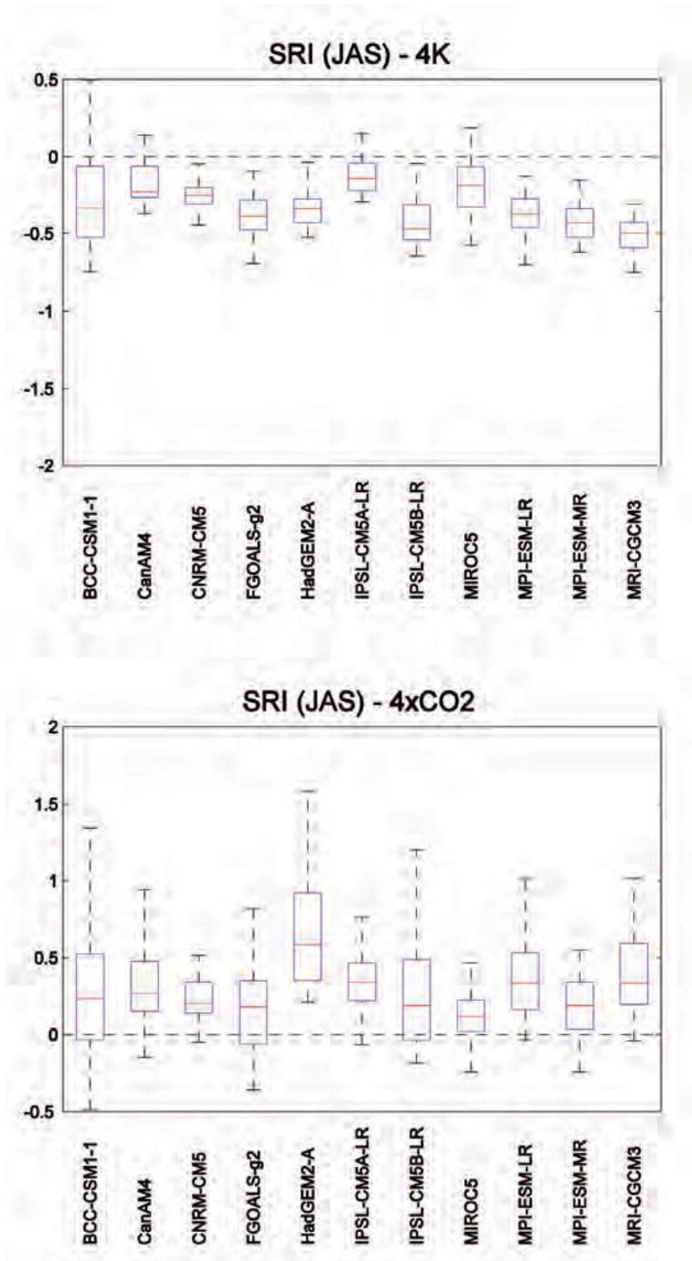

Box plot of the SRI changes in the idealized sensitivity experiments relative to CTL (Δ = (Exp – CTL) / |CTL|). In each box, the central mark is the median, the edges of the box are the 25th and 75th percentiles, and the whiskers extend to the most extreme data points.

Table 2. Sensitivity of the Sahelian precipitation to global warming in the 4K and $4xCO_2$ experiments.

Model	4K	$4xCO_2$	Ratio
BCC-CtSM1-1	-0.0678	0.5754	8.49
CanAM4	-0.0951	1.2682	13.34
CNRM-CM5	-0.2428	1.9412	8.00
FGOALS-g2	-0.1642	0.5282	3.22
HadGEM2-A	-0.0898	2.1713	24.18
IPSL-CM5A-LR	-0.0591	1.5311	25.91
IPSL-CM5B-LR	-0.0929	0.4781	5.15
MIROC5	-0.2001	0.9134	4.56
MPI-ESM-LR	-0.1937	1.8522	9.56
MPI-ESM-MR	-0.2552	1.0659	4.18
MRI-CGCM3	-0.1395	1.3075	9.37

A Global Warming (GW) index is computed by averaging the surface air temperature in the band [50°S-70N], and the sensitivity is estimated through the ratio between the SRI response and the GWs in the idealized experiments compared to control simulations (CTL). Third column: ratio of the two sensitivity coefficients ($4xCO_2$/4K).

NAT being particularly weak. HadGEM2-A shows SAT to be three times more important than NAT, whereas all other models show NAT to be six to as much as 80 times more important than SAT (not shown). This suggests a specific high sensitivity of the Sahelian precipitation to the regional-versus-global thermal forcing in HadGEM2-A compared to the other models, which might favor the regional scale GHG radiative heating impact compared to the global scale SST heating impact.

Second, the response of the same models to changes in SST and GHG forcings was studied by analyzing two idealized experiments aiming at emphasizing the responses through the simulation of extreme conditions, one with a 4K homogeneous increase in global SST, and the other having a fourfold increase in atmospheric CO_2 concentration. By analyzing the SRI responses, it appears that the HadGEM2-A response to 4K SST is in line with most of the model ensemble, while in the $4xCO_2$ experiment, the HadGEM2-A shows the strongest response compared to the other models (see figure on left). The SRI sensitivity summarized in Table 2 in the 4K experiment is in the range -0.26 to -0.06 mm/day/K, with the HadGEM2-A response close to the lower limit (-0.09 mm/day/K). On the other hand, in the $4xCO_2$ experiment, the sensitivity is in the range 0.48–2.17 mm/day/K, and the HadGEM2-A is at the upper limit, showing the strongest response compared to the other models (figure on left). HadGEM2-A also has the second highest ratio of relative sensitivity of $4xCO_2$/4K, well above the other models (third column of Table 2).

Possible Contribution of Internal Variability

Another issue that should be considered is the range of atmospheric-only internal variability and its possible contribution to the recent Sahel rainfall recovery. In an Atmospheric Model Intercomparison Project (AMIP)-type simulation ensemble

that is different from the repeating SST-forced experiments of Dong and Sutton, five members of the IPSL-CM5A-LR model predicted a Sahel rainfall recovery from the 1980s–2000s but with large internal variability, ranging from +6% to +21% (Figure 3b of Roehrig et al.). Other 100-year simulations of the same IPSL model forced by either the 1955–1965 or the 1975–1985 mean SST global pattern show a high variation of the 10-year running means of Sahel rainfall along each of the 100-year periods, close to 20% between the highest and the lowest running means (F. Hourdin, personal communication). That means that decadal scale variability (at least for 10-year sequences) due to the atmosphere alone is high over the Sahel and might be responsible for a significant part of the recent Sahel rainfall recovery.

The Need for a Process-Based Assessment: Example of the Saharan Heat Low

To better understand the diversity of West African monsoon sensitivity in climate models, it is necessary to address some of the key processes in play. In summer, the Saharan heat low (SHL), combined with the high-pressure southward, produces a low-level pressure gradient that controls the West African monsoon. The warmer the Sahara is, the stronger the thermal depression becomes and the more intense the monsoon flow leading to enhanced convection over the central and eastern Sahel and weaker convection over the western Sahel (Lavaysse et al., 2010). In this context, Cook and Vizy (2015) show by using three reanalysis products that the recent recovery in Sahel rainfall is concomitant with the increase of Sahara surface temperature that is 2-4 times greater than that of the tropical-mean temperature. It is accompanied by a strengthening of both the Saharan heat low and the African easterly jet. This amplified warming, confined to the lower troposphere, seems to be due to large increases in both downward and upward longwave radiation. The contribution of atmospheric carbon dioxide increase and water vapor increase in this warming is probable. However uncertainties in the surface heat balance remain large in reanalysis products due to the sparse ground-based observations over the desert and to poor representation of the radiative properties of aerosols and of the surface reflectivity in this arid region. Evan et al. (2015) also addressed the origins of the recent recovery from the Sahel drought, showing that the temperature increase in the SHL over the last 30 years was forced by anomalous nighttime longwave heating of the surface by water vapor. They identified a Saharan water vapor–temperature feedback associated with an increase in the low-level water vapor convergence within the SHL as SHL temperatures rise. The structure of the drought recovery is consistent with a warming SHL and is evidence of a fundamental, but not exclusive, role of the SHL in the recent increase in Sahelian monsoon rainfall.

Regarding climate simulations, Biasutti et al. (2009) highlighted the role of SHL with a better understanding of the source of discrepancy in CMIP3 Sahel rainfall projections. Lavaysse et al. (2015) showed that despite a large variability in CMIP5 AMIP simulations over the last 30 years within a set of 15 climate models, the warming trend in SHL is observed in the models' ensemble mean. These climate models represent the West African monsoon interactions with SHL pulsations quite differently; however, some of them are able to simulate an accurate rainfall-SHL regression pattern, or a zonal rainfall anomaly pattern, with more precipitation over the Central Sahel and less precipitation over the western Sahel associated with the long-term SHL increase. Projections of future climate over the Sahel in CMIP5 runs are qualitatively consistent with this recent evolution and this zonal dipole is associated with a continuing increase of temperature in the SHL (Monerie et al., 2012). James et al. (2015) explained the simulated drying over the western Sahel by anomalous subsidence at 400 hPa, possibly associated with the SHL warming that may be responsible for increases in dry convection with potential feedbacks on the monsoon and the African easterly jet. However, they questioned the accuracy of this modeled circulation mode, as it is not clear in reanalysis products what different mechanisms are used for drying in the western Sahel.

Addressing the possible role of GHG increases in the recent recovery in Sahel rainfall requires more process-based assessments on ensembles of both historical simulations and future climate projections. This will help reduce uncertainties over this region and provide well-founded expert judgements of the trustworthiness of climate model projections to decision-makers, which is one of the objectives of the new African Monsoon Multidisciplinary Analysis (AMMA)-2050 Project (Department for International Development-Natural Environment Research Council Future Climate For Africa project 2015–2019). However, there are still weaknesses in our understanding of atmospheric processes in this region. Data from recent short-term AMMA field campaigns, as well as other affiliated campaigns over West Africa and the surrounding oceans, are potentially valuable resources. Moreover, the maintenance of long-term monitoring of the hydrological cycle over West Africa is critical to detect possible trends and attribute their causes.

References

Biasutti, M., A.H. Sobel and S.J. Camargo, 2009. The role of the Sahara heat low in summertime Sahel rainfall variability and change in the CMIP3 models. *J. Clim.*, 22, 5755-5770.

Biasutti, M., 2013. Forced Sahel rainfall trends in the CMIP5 archive. *J. Geophys. Res. Atmos.*, 118, 1613–1623.

Bony, S., G. Bellon, D. Klocke, S. Sherwood, S. Fermepin and S. Denvil, 2013. Robust direct effect of carbon dioxide on tropical circulation and regional precipitation. *Nat. Geosci.*, 6, 447–451.

Caminade, C., and L. Terray, 2010. Twentieth century Sahel rainfall variability as simulated by the ARPEGE AGCM, and future changes. *Clim. Dynam.*, 35, 75–94.

Cook, K.H., and E.K. Vizy, 2006. Coupled model simulations of the West African monsoon system: Twentieth- and twenty-first-century simulations. *J. Clim.*, 19, 3681–3703.

Cook, K.H., and E.K. Vizy, 2015. Detection and analysis of an amplified warming of the Sahara desert. *J. Clim.*, 28, 6560-6580.

Dong, B., and R. Sutton, 2015. Dominant role of greenhouse-gas forcing in

the recovery of Sahel rainfall. *Nat. Clim. Change*, 5, 757-760.

Evan, A.T., C. Flamant, C. Lavaysse, C. Kocha and A. Saci, 2015. Water vapor-forced greenhouse warming over the Sahara desert and the recent recovery from the Sahelian drought. *J. Clim.*, 28, 108-123.

Gaetani, M., C. Flamant, S. Bastin, S. Janicot, C. Lavaysse, F. Hourdin, P. Braconnot and S. Bony, 2015. Climate Dynamics West African Monsoon dynamics and precipitation: The competition between global SST warming and CO_2 increase in CMIP5 idealized simulations. *Clim. Dynam.*, in revision.

Giannini, A., 2010. Mechanisms of climate change in the semiarid African Sahel: The local view. *J. Clim.*, 23, 743–756.

Giannini, A., S. Salack, T. Lodoun, A. Ali, A.T. Gaye and O. Ndiaye, 2013. A unifying view of climate change in the Sahel linking intra-seasonal, interannual and longer time scales. *Environ. Res. Lett.*, 8, 024010.

Giannini, A., 2015. Climate change comes to the Sahel. *Nat. Clim. Change*, 5, 720–721.

Haarsma, R.J., F.M. Selten, S.L. Weber and M. Kliphuis, 2005. Sahel rainfall variability and response to greenhouse warming. *Geophys. Res. Lett.*, 32, 1–4.

Held, I.M., T.L. Delworth, J. Lu, K.L. Findell and T.R. Knutson, 2005. Simulation of Sahel drought in the 20th and 21st centuries. *Proc. Natl. Acad. Sci. U.S.A.*, 102, 17891–17896.

Hoerling, M., J. Hurrell, J. Eischeid and A. Phillips, 2006. Detection and attribution of twentieth-century northern and southern African rainfall change. *J. Clim.*, 19, 3989–4008.

James, R., R. Washington and R. Jones, 2015. Process-based assessment of an ensemble of climate projections for West Africa. *J. Geophys. Res.*, 120, 1221-1238.

Lavaysse, C., C. Flamant and S. Janicot, 2010. Regional-scale convection patterns during strong and weak phases of the Saharan heat low. *Atmos. Sci. Lett.*, 11, 255-264.

Lavaysse, C., C. Flamant, A. Evan, S. Janicot and M. Gaetani, 2015. Recent climatological trend of the Saharan heat low and its impact on the West African climate. *Clim. Dynam.*, doi:10.1007/s00382-015-2847-z.

Lebel, T. and A. Ali, 2009. Recent trends in the Central and Western Sahel rainfall regime (1990-2007). *J. Hydrol.*, 375, 52-64.

Mohino, E., S. Janicot and J. Bader, 2011. Sahel rainfall and decadal to multi-decadal sea surface temperature variability. *Clim. Dynam.*, 37, 419–440.

Monerie, P.-H., B. Fontaine and P. Roucou, 2012. Expected future changes in the African monsoon between 2030 and 2070 using some CMIP3 and CMIP5 models under a medium-low RCP scenario. *J. Geophys. Res.*, 117, doi:10.1029/2012JD017510.

Panthou, G., T. Vischel and T. Lebel, 2014. Recent trends in the regime of extreme rainfall in the Central Sahel. *Int. J. Climatol.*, 34, 3998-4006.

Roehrig, R., D. Bouniol and F. Guichard, 2013. The present and future of West African monsoon: A process-oriented assessment of CMIP5 simulations along the AMMA transect. *J. Clim.*, 26, 6471–6505.

Taylor, K.E., R.J. Stouffer and G.A. Meehl, 2012. An overview of CMIP5 and the experiment design. *Bull. Am. Meteor. Soc.*, 93, 485–498.

Vizy, E.K., K.H. Cook, J. Crétat and N. Neupane, 2013. Projections of a wetter Sahel in the twenty-first century from global and regional models. *J. Clim.*, 26, 4664-4687.

Meeting/Workshop Reports

Workshop on Uncertainties at 183 GHz

Paris, France
29-30 June 2015

Hélène Brogniez[1], Stephen English[2] and Jean-François Mahfouf[3]

[1]Laboratoire Atmosphères, Milieux, Observations Spatiales (LATMOS), Guyancourt, France; [2]European Center for Medium-Range Weather Forecasting, Reading, UK; [3]Centre National de Recherches Météorologiques/Météo-France, Toulouse, France

Thirty-eight scientists from 19 institutes attended the Workshop to discuss the uncertainties of radiometric observations at 183 GHz. These observations are among the most important sources of humidity information for global and regional analyses, weather forecasts and climate monitoring. A sound characterization of their absolute calibration is important for their effective use in models. Recent cross-comparisons between the existing microwave sounders, Sondeur Atmospheric du Profil d'Humidité Intertropical par Radiométrie (SAPHIR, on Megha-Tropiques), the Advanced Technology Microwave Sounder (ATMS; on Suomi-National Polar-orbiting Partnership missions), the Special Sensor Microwave Imager/Sounder [SSMIS, on Defense Meteorological Satellite Program (DMSP)-F17 and F18)] and the Microwave Humidity Sounder (MHS on MetOp-A and B and National Oceanic and Atmospheric Administration-18 and -19), show a very good consistency among them, well within the radiometric noises of the instruments. However, when the measurements are simulated in a numerical weather prediction (NWP) system, or compared to radiative transfer model (RTM) calculations that use radiosonde (RAOBS) profiles of temperature and humidity, a channel-dependent bias, which increases from the center to the wings of the 183 GHz line, is observed. The figure on page 16 clearly shows this pattern.

The workshop was organized around three main objectives: (1) describe the biases and separate those that are common to all approaches from those that may have resulted from a particular methodology; (2) identify and, where possible, quantify uncertainty in every component of the comparison; and (3) where possible, begin the process of attribution of the biases, which may in due course lead to their elimination. To address these ambitious goals, experts in many different aspects of the problem were assembled. This included specialists in RAOBS calibration, NWP models and data assimilation, instrument biases and radiative transfer models (both the models themselves and the underlying spectroscopy). Comparisons were also undertaken with other techniques for sensing humidity information, such as the Global Navigation Satellite Systems (GNSS), Differential Absorption Lidar (DIAL), Raman Lidar, and infrared (IR) radiances.